1
Introduction

1.1 Pairing in nuclei, superconductors, liquid ^{3}He and neutrons stars

If one sweeps a magnetic field through a metallic ring (e.g. a ring made out of lead) immersed in liquid helium ($T \sim 4\,\mathrm{K}$) it induces a current which does not show any measurable decrease for a year, and a lower bound of 10^5 years for its characteristic decay time has been established using nuclear resonance to detect any slight decrease in the field produced by the circulating current (File and Mills (1963)). If a torus-shaped vessel filled with liquid helium below the critical temperature $T_c = 2.17\,\mathrm{K}$ (known as He II) and packed with porous material, which provides very narrow capillary channels, is rotated around its axis of symmetry and then brought to rest, the liquid continues to flow (Reppy and Depatie (1964)), showing no reduction in the angular velocity over a twelve-hour period, and indicating that He II can flow without dissipation. Using an adiabatic cooling apparatus, Osheroff *et al*. (1972 a,b) found two anomalies in the pressure–time curve of liquid ^{3}He, when the volume was changed at a constant rate. At the critical temperature $T_c = 2.7\,\mathrm{mK}$ the slope of the curve suffered a discontinuity, and at about $T_c = 1.8\,\mathrm{mK}$ there was a singularity involving hysteresis (see also Osheroff (1997) and Lee (1997)). If a deformed nucleus in its ground state is set into a state of rotation by the action of a non-uniform, time-dependent Coulomb field, it displays rotational bands with a moment of inertia which is a fraction (between one-half to one-third) of the rigid moment of inertia (Belyaev (1959), Bohr and Mottelson (1975)). Rotating neutron stars (pulsars) display marked glitches, that is, sudden increases in the frequency of the emitted pulses of radiation (McKenna and Lyne (1990), McCullough *et al*. (1990), Flanagan (1990), Anderson *et al*. (1982)). All the above observations are examples of phenomena known as superconductivity and superfluidity.

From a microscopic point of view, helium atoms are structureless spherical particles interacting via a two-body potential. The attractive part of this potential,

https://doi.org/10.1017/9781009401920.002 Published online by Cambridge University Press

arising from weak Van der Waals-type dipole, quadrupole, etc. forces, causes helium gas to condense, at normal pressure, into a liquid at temperatures of 3.2 K and 4.2 K for ^{3}He and ^{4}He respectively.

The striking difference in the behaviour of ^{3}He and ^{4}He at even lower temperatures, in particular the fact that the critical temperature for ^{3}He to become superfluid is roughly one thousandth of the transition temperature of ^{4}He, is a consequence of the fact that ^{3}He is composed of an odd number of fermions (two protons, one neutron and two electrons), and is thus also a fermion, while ^{4}He, containing one more neutron, is a boson. Since in a Bose system single-particle states may be multiply occupied, at low temperatures this system has a tendency to condense into the lowest-energy single-particle state (Bose–Einstein condensation). It is believed that the superfluid transition in ^{4}He is a manifestation of Bose–Einstein condensation (see e.g. Leggett (1989), Pitaevskii and Stringari (2003), Pethick and Smith (2002)).

The basic feature of the Bose condensate is its phase rigidity, i.e. the fact that it is energetically favourable for the particles to condense into a single-particle state of fixed quantum-mechanical phase, such that the global gauge symmetry is spontaneously broken. For three-dimensional (3D-) systems, macroscopic flow of the condensate is (meta) stable, giving rise to the phenomenon of superfluidity (frictionless flow).

In a Fermi system, on the other hand, the Pauli exclusion principle allows only single occupation of fermion states. In the simplest approximation the fermions move independently in an average potential and occupy the lowest available single-particle states up to a Fermi energy ε_F. Fermions with energy near ε_F are, in a variety of systems, subject to a pairing residual interaction. The associated pairing correlations are important for understanding the structure of the low-lying states of nuclei, the properties of neutron stars and those of metals and of liquid helium ^{3}He at low temperatures. The relevant fermions are nucleons in nuclei, and in neutron stars, electrons in superconductors and ^{3}He atoms in liquid helium.

The pairing interaction leads to pairs of fermions bound in states coupled to integer spin (zero or one). These pairs, whose structure is different for each physical system, behave like bosons, and can at low temperatures Bose-condense, the condensate being characterized by macroscopic quantum coherence leading to the superconducting or superfluid phase. The mechanism and the consequences of this condensation in the case of nuclei is the subject of the present monograph.

Particular emphasis is placed on the study of quantal-size-effects (QSE). These effects are due to the fact that the nucleus is a finite many-body system where the surface plays a paramount role. In fact, the nuclear surface is not only the source of space quantization and thus of the discreteness of the single-particle levels, but also, by vibrating as a whole, of the existence of collective surface modes. Furthermore, because the length at which Cooper pairs are correlated is much larger than the nuclear dimension, the nuclear superfluid can be viewed as a zero-dimensional system. Because the number of pairs which build the condensate is small, fluctuations become very important.

1.2 Macroscopic wavefunction and phase rigidity

The central idea of the macroscopic quantum state is represented by assigning a macroscopic number of particles to a single wavefunction ($\tilde{\Psi}$) (see e.g. Anderson (1964, 1984), Mercerau (1969), Tilley and Tilley (1974), Bruus and Flensberg (2004)). These particles are assumed to have condensed into a single state. This condensation results in a macroscopic density of particles (ρ_{s}) sharing the same quantum phase (Φ). The resulting wavefunction is then $\bar{\Psi} = \Psi \exp(\mathrm{i}\Phi)$. In this form $\rho_{\mathrm{s}} = (\bar{\Psi}^* \bar{\Psi})$ is not the usual probability of finding a particle but, owing to the macroscopic number of particles involved, is actually the effective particle density. Both Ψ and Φ may be functions of space and time and their variations will therefore determine the motion of the quantum fluid.

In what follows we shall be more interested in understanding the consequences the r-dependence of Φ has on the behaviour of the system and somewhat neglect the r-dependence of Ψ. Since, by definition, the particles are in precisely the same state and must therefore behave in an identical fashion, the equations of motion for the macrostate must also be identical to the equations of motion for any single particle in this state. Because the phase is common to so many particles, its effects do not average out on a macroscopic scale, but remain to fundamentally determine the behaviour of the system.

Changes in the wavefunction are of course determined by the Schrödinger equation. In particular, the centre of mass velocity ($\vec{V}$) can be calculated for this wavefunction from the velocity operator ($\vec{v}$) common to all the particles

$$\vec{v} = -\frac{1}{m^*}(\mathrm{i}\hbar\vec{\nabla} + e^*\vec{A})$$

where e^* and m^* are, respectively, the (effective) charge and mass of the particles and $\vec{A}$ is the vector potential. The centre of mass velocity is

$$\vec{V} = \tfrac{1}{2}\left\{\bar{\Psi}\vec{v}^{\,+}\bar{\Psi}^{\,+} + \bar{\Psi}^{\,+}\vec{v}\bar{\Psi}\right\} / \left(\bar{\Psi}^{\,+}\bar{\Psi}\right)$$

giving a current

$$\vec{J} = e^*\rho_{\mathrm{s}}\vec{V} = \frac{e^*\rho_{\mathrm{s}}}{m^*}\left(\hbar\vec{\nabla}\Phi - e^*\vec{A}\right). \tag{1.1}$$

By taking the curl of this equation one can derive another equation of significance, namely

$$\vec{\nabla} \times \vec{J} + \frac{\rho_{\mathrm{s}}e^{*2}}{m^*c}\vec{B} = 0. \tag{1.2}$$

https://doi.org/10.1017/9781009401920.002 Published online by Cambridge University Press

This is the solution found by F. London and H. London (London, 1954) of the relation

$$\frac{\partial}{\partial t}\left(\vec{\nabla}\times\vec{J}+\frac{\rho_{\mathrm{s}}{e^*}^2}{m^*c}\vec{B}\right)=0. \tag{1.3}$$

This equation together with the Maxwell equation

$$\vec{\nabla}\times\vec{B}=\frac{4\pi}{c}\vec{J}, \tag{1.4}$$

characterizes a medium that conducts electricity without dissipation. In fact, in such circumstances, electrons under the effect of an electric field will be freely accelerated without dissipation so that their mean velocity $\vec{v}_{\mathrm{s}}$ will satisfy

$$m^*\frac{\mathrm{d}\vec{v}_{\mathrm{s}}}{\mathrm{d}t}=-e^*\vec{E}.$$

Since the current density carried by these electrons is $\vec{J}=-e^*v_{\mathrm{s}}\rho_{\mathrm{s}}$, the above equation can be written as

$$\frac{\mathrm{d}}{\mathrm{d}t}\vec{J}=\frac{\rho_{\mathrm{s}}e^{*2}}{m^*}\vec{E}. \tag{1.5}$$

The Fourier transform of this equation gives the ordinary AC conductivity for an electron gas of density ρ_{s} in the Drude model, when the relaxation time τ becomes infinitely large, that is,

$$\vec{J}=\sigma_{\mathrm{s}}(\omega)E(\omega)$$

where

$$\sigma_{\mathrm{s}}(\omega)=\lim_{\tau\to\infty}\sigma(\omega)$$

is the frequency dependent (or AC) conductivity

$$\sigma(\omega)=\frac{\sigma_0}{1-\mathrm{i}\omega\tau},$$

the zero-frequency conductivity being

$$\sigma_0=\frac{\rho_{\mathrm{s}}{e^*}^2\tau}{m^*}.$$

Substituting equation (1.5) into Faraday's induction law

$$\nabla\times\vec{E}=-\frac{1}{c}\frac{\partial\vec{B}}{\partial t},$$

one finds equation (1.3). In other words, $\vec{\nabla}\times\vec{J}+\frac{\rho_{\mathrm{s}}e^{*2}}{m^*c}\vec{B}=C$ characterizes a non-dissipative electric medium. The more restrictive London equation, which

https://doi.org/10.1017/9781009401920.002 Published online by Cambridge University Press

specifically characterizes superconductors and distinguishes them from mere perfect conductors, requires in addition $C = 0$.

The reason for replacing (1.3) by (1.2) is that the latter equation leads directly to essential experimental facts, by forbidding currents or magnetic fields internal to the superconductor except within a layer of thickness $\Lambda = \left(\frac{m^* c^2}{4\pi \rho_s e^{*2}}\right)^{1/2} \approx 42 \left(\frac{r_s}{a_0}\right)^{3/2} \left(\frac{\rho}{\rho_s}\right)^{1/2}$ (London penetration depth) of the surface, $r_0 = a_B r_s$ being the Wigner-Seit cell radius of the system under consideration, defining the density ρ ($r_0 = (4\pi\rho/3)^{-1/3}$). In fact, equations (1.2) and (1.4) imply

$$\nabla^2 \vec{B} = \frac{4\pi \rho_s e^{*2}}{m^* c^2} \vec{B},$$
$$\nabla^2 \vec{J} = \frac{4\pi \rho_s e^{*2}}{m^* c^2} \vec{J},$$

where the relation $\vec{\nabla} \times (\vec{\nabla} \times) = \vec{\nabla}(\vec{\nabla} \cdot) - \nabla^2$ was used. Assuming a semi-infinite superconductor occupying the half space $x > 0$,

$$B(x) = B(0) e^{-x/\Lambda},$$

and

$$J(x) = J(0) e^{-x/\Lambda}.$$

Thus, the London equation implies the Meissner effect, along with a specific picture of the surface currents that screen out the applied field. These currents occur within a surface layer of thickness $10^2 - 10^3$ Å. Within this same surface layer the field drops continuously to zero, predictions which are confirmed, among other things, by the fact that the field penetration is not complete in superconducting films as thin as or thinner than the penetration depth Λ.

Let us now return to equation (1.1). This relation can be obtained by minimizing the free energy of the system with respect to the phase Φ. In other words, subject to a phase gradient, the system minimizes its energy by carrying a current even in thermodynamical equilibrium, and such a current is always dissipationless. This is true both for charged systems (like, e.g., metals where $e^* = 2e$ and $m^* = 2m_e$), as well as for neutral systems (like, e.g., He II, where $e^* = 0$ and $m^* = m_4$).

Of course there is an energy cost for the system to carry the current, but as long as this cost is smaller than the alternative which is to go out of the superfluid or superconducting state, the current carrying state is chosen. The critical current is reached when the energies are equal (and equal to the value of the gap, see Sections 1.4 and 1.5 and Figs. 1.6 and 1.7), and then the superfluid or superconductor goes into the normal state (see equations (1.17) and (1.21), respectively).

Within this context, it should be noted that the appearance of the excitation gap is not the reason for the superfluidity or superconductivity itself, but a consequence of the spontaneous symmetry breaking of gauge invariance. In fact, gapless superconductors do exist (in this connection see Sections 5.3 and 6.2.1).

1.3 Broken symmetry and collective modes

In many phase transitions, such as that to the ferromagnetic state, or from the normal to the superconducting state, or again from a spherical to a deformed nucleus, the ground state of the low-temperature phase has a lower symmetry than the Hamiltonian used to describe the system. The situation is one of broken symmetry. In cases where the symmetry group that is broken is continuous (e.g. the rotation group), a new collective mode appears, whose frequency, in the absence of long-range forces, goes to zero in the long wavelength limit (Anderson Goldstone Nambu (AGN) mode (see Chapter 4)). For the ferromagnet, the elementary excitations required by Goldstone's theorem (Goldstone, 1961) are Bloch's spin waves (magnons), in which the magnetization precesses about its direction in the ground state (see Figs. 1.1 and 1.2).

Superconductors furnish an example of a system in which the excitations required by the symmetry-breaking process have a finite frequency in the

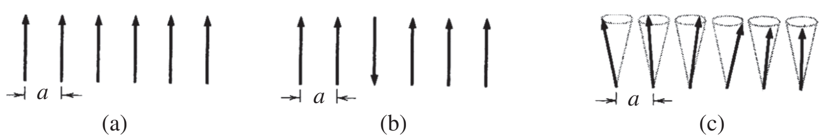

Figure 1.1. (a) Classical picture of the ground state of a simple ferromagnet; all spins are parallel. (b) A possible excitation; one spin is reversed. (c) The low-lying elementary excitations are spin waves. The ends of the spin vectors precess on the surfaces of cones, with successive spins advanced in phase by a constant angle (after C. Kittel (1968)). From *Introduction to Solid State Physics*, 7th edition, by Charles Kittel, Copyright 1995 John Wiley & Sons Inc. Reprinted with permission of John Wiley & Sons Inc.

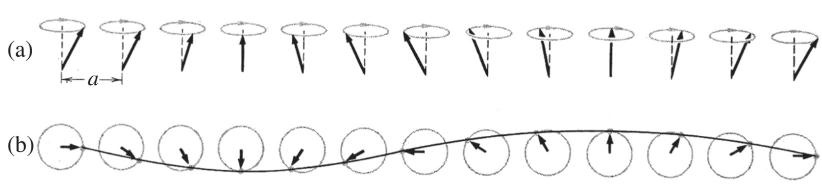

Figure 1.2. A spin wave on a line of spins. (a) The spins viewed in perspective. (b) Spins viewed from above, showing one wavelength. The wave is drawn through the ends of the spin vectors (after Kittel (1968)). From *Introduction to Solid State Physics*, 7th edition, by Charles Kittel, Copyright 1995 John Wiley & Sons Inc. Reprinted with permission of John Wiley & Sons Inc.

https://doi.org/10.1017/9781009401920.002 Published online by Cambridge University Press

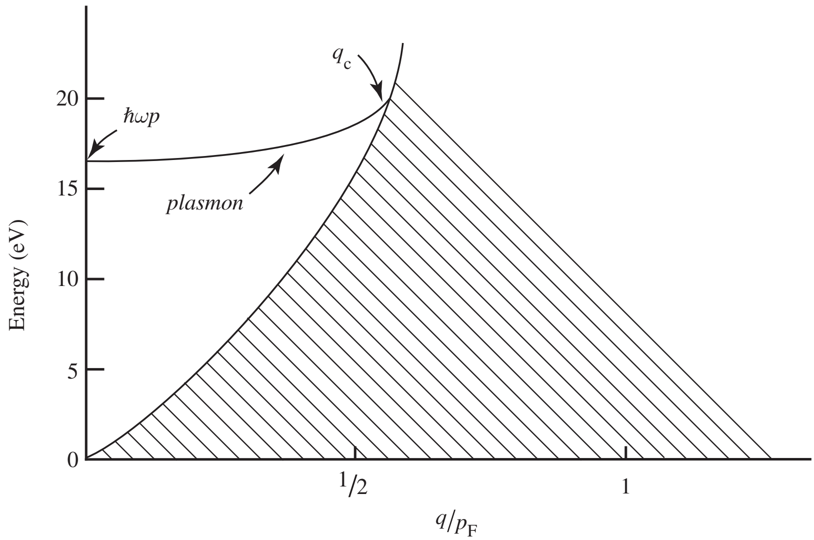

Figure 1.3. Excitation spectrum of density fluctuations in a quantum plasma with the density of Al, as calculated in the random phase approximation. Plasmons are essentially undamped (see also Section 8.3.4) for wavevectors less than q_c, and are strongly damped (Landau damping) beyond q_c by the single particle–hole excitations, whose energies lie within the hatched region (after Pines (1963)).

long wavelength limit (because of the infinite range of the Coulomb force): the corresponding Goldstone mode is the familiar plasma oscillation (see Fig. 1.3).

For a neutral fermion superfluid, on the other hand, the collective mode is the zero-sound mode proposed by Anderson (1958) and Bogoliubov (1958a), which has a vanishing frequency at long wavelengths (see Section 4.3.1).

An example of AGN boson in a neutral system is provided by the fourth sound in superfluid ^{3}He, which corresponds to the oscillatory motion of the superfluid phase in a confined geometry (superleak) where the normal fluid is clamped. For example, assume a porous medium. In it, the normal-fluid fraction (see equation (1.12)) is clamped by the scattering of quasiparticles with the surface of the very narrow channels. The superfluid fraction is barely affected by the confining walls, provided that the channel diameter is greater than the coherence length $\xi(T)$ (equation (1.32)), and thus may move freely. The oscillatory motion of the superfluid phase in such a confined geometry is called fourth sound (see Vollhardt and Wölfle (1990)). In the case of atomic nuclei, the very occurrence of collective rotational degrees of freedom may be said to originate in a breaking of rotational invariance, which introduces a ‘deformation’ that makes it possible to specify an orientation of the system (Bohr and Mottelson, 1975). Rotation (see Fig. 1.4) represents the collective mode associated with such a spontaneous

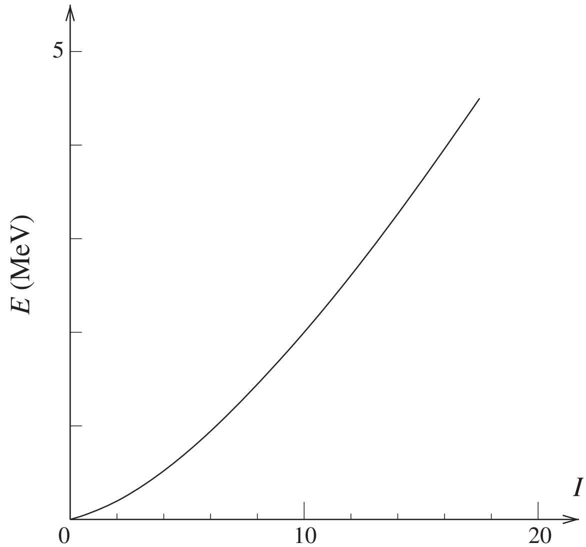

Figure 1.4. Schematic representation of the (discrete) energy levels of the (ground state) rotational band of a quadrupole deformed atomic nucleus as a function of the angular momentum I ($E = (\hbar^2/2\mathcal{I})I(I+1)$, where $\mathcal{I}$ is the moment of inertia).

symmetry breaking (AGN boson). The full degrees of freedom associated with rotations in three-dimensional space come into play if the deformation completely breaks the rotational symmetry, thus permitting a unique specification of the orientation. If the deformation is invariant with respect to a subgroup of rotations, the corresponding elements are part of the intrinsic degree of freedom, and the collective rotational modes of excitation are correspondingly reduced, disappearing entirely in the limit of spherical symmetry.

1.4 Superfluid ^{4}He (He II)

^{4}He becomes liquid under its own vapour pressure at 4.21 K. The liquid phase at this temperature, helium I, behaves like a normal liquid, but at 2.17 K it shows a further phase transition – to helium II. Helium II is a most peculiar liquid: it shows superfluidity, i.e. a lack of viscosity when flowing through a narrow slit or capillary. At 2.17 K the specific heat shows a very strong pronounced peak, resembling the Greek letter λ, whence Ehrenfest suggested the name λ-point for the transition point (see Fig. 1.5).

The theory developed by Landau (Landau (1941, 1947)) was constructed upon the basic idea that the equilibrium properties of liquid helium below the λ-point could be expressed in terms of the energy spectrum of the elementary

https://doi.org/10.1017/9781009401920.002 Published online by Cambridge University Press

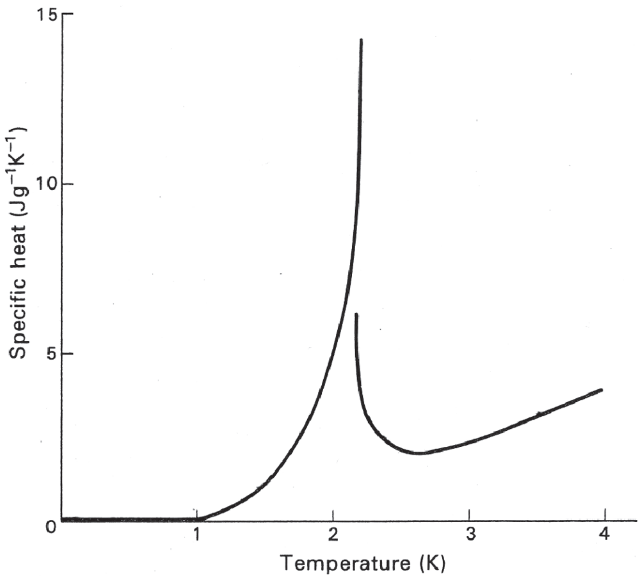

Figure 1.5. Specific heat of ^{4}He (after Atkins (1959)).

excitations possible in helium, namely phonons and rotons. Landau considers the quantization of liquids and reaches the conclusion that there are states possible in the liquid for which

$$\text{curl}\,\vec{v} = 0, \tag{1.6}$$

where $\vec{v}$ is the velocity of the liquid. Note that this relation is obtained from equation (1.1) for $e^* = 0$ (neutral system). Such states correspond to potential flow, as would be the case in classical hydrodynamics, because, just as there is no continuous transition in quantum mechanics between states with zero angular momentum and with non-vanishing angular momentum, in the same way there may be no continuous transition between states with curl $\vec{v} = 0$ and those with curl $\vec{v} \neq 0$. Consequently, one concludes that there will be an energy gap Δ between the lowest energy level corresponding to potential flow and the lowest energy level of vortex motion (curl $\vec{v} \neq 0$). In order that the liquid be superfluid, it is necessary that the vortex motions start at a higher energy than the potential flow motions.

The spectrum of helium II can thus be seen as a superposition of two continuous spectra: one corresponding to potential flow and one corresponding to vortex motion. The potential flow part of the spectrum corresponds to longitudinal waves, i.e. sound waves. The elementary excitations are thus phonons, the energy

https://doi.org/10.1017/9781009401920.002 Published online by Cambridge University Press

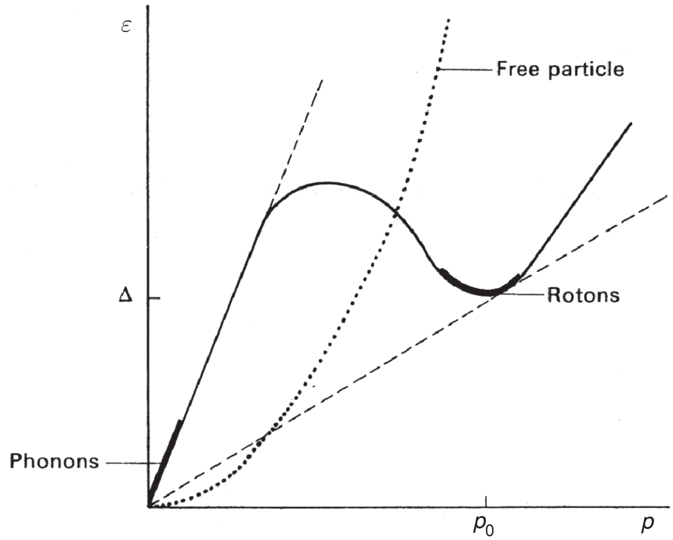

Figure 1.6. Phonon–roton spectrum suggested by Landau. Broken lines indicate superfluid critical velocities. Dotted line shows free-particle parabola for comparison.

spectrum of which is known to be (Fig. 1.6)

$$\varepsilon_{\text{ph}} = c_{\text{s}} p,$$

where p is the momentum of the excitation while c_{s} is the sound velocity.

The elementary excitations of the vortex motion were called rotons by Tamm. The roton spectrum is given by

$$\varepsilon_{\text{r}} = \Delta + \frac{(p - p_0)^2}{2\mu}, \tag{1.7}$$

where Δ is the energy gap mentioned above while μ is the inertia of the rotons.

It should be emphasized that the above two equations (see also Fig. 1.6) give the energy of the excitation spectrum of the elementary excitations of the helium II and not the energy spectrum of the single helium atoms

$$\varepsilon_{\text{sp}} = \frac{p^2}{2m_4}.$$

Note that given the dispersion relation shown in Fig. 1.6 it is difficult to speak strictly of rotons and phonons as qualitatively different types of excitations. It could be more correct to speak simply of the long wave (small p) and short wave (p in the neighbourhood of p_0) excitations. In any case, there is an essential difference between phonons and rotons. Phonons can have zero energy in the long wavelength limit and thus qualify as AGN modes (Anderson (1952, 1963), Nambu (1959, 1960)), while rotons have always an energy $\geq \Delta$ and can thus

https://doi.org/10.1017/9781009401920.002 Published online by Cambridge University Press

never be an example of Goldstone's theorem (Goldstone (1961), Goldstone *et al.* (1962)).

At finite temperature and assuming it to be sufficiently low, one can consider the excitation of He II to be that of a perfect gas of phonons and rotons. This means that one neglects the interaction between the elementary excitations. If one assumes that the presence of excitations does not affect the spectrum of any new excitation, one can prove (see below) that new phonon and rotons cannot be excited if the liquid moves with $V < (V_c)_{\text{phon,rot}}$ (see equations (1.17) and (1.19)) through a capillary. However, the phonon and roton gas will not be superfluid. Landau showed indeed that this gas will stick to the walls and behave like an ordinary liquid. This leads to the conclusion that at finite, not too high, temperatures, part of the liquid behaves normally while the remainder shows superfluidity.

In other words in a quantum liquid such as helium both normal and superfluid motion can occur and while there is no real division of the liquid into two parts, such that some atoms belong to the superfluid liquid and others to the normal liquid, it is possible to assign to each of the two liquids its own mass. In fact, the density of the normal liquid at a given temperature can be defined as the effective mass of the roton and phonon gases.

To evaluate these masses, we consider the liquid moving at a velocity $\vec{V}$. Since the phonons are bosons, their distribution function is $\{\exp \beta[\varepsilon - (\vec{p} \cdot \vec{V})] - 1\}^{-1}$, where $\beta = 1/T$. The total momentum per unit volume is then

$$\vec{P_{\text{ph}}} = \frac{1}{(2\pi h)^3} \int \frac{\vec{p}\, \mathrm{d}^3 p}{\mathrm{e}^{\beta[\varepsilon - \vec{p}\cdot\vec{V}]} - 1}. \tag{1.8}$$

The effective phonon mass density ρ_{ph} can then be defined through the relation

$$\vec{P_{\text{ph}}} = \rho_{\text{ph}} \vec{V}. \tag{1.9}$$

For small $\vec{V}$ one can expand the denominator in the integral and retain only the linear term in $\vec{V}$. This leads to

$$\rho_{\text{ph}} = \frac{4}{3} \rho \frac{E_{\text{ph}}}{c_{\text{s}}^2}, \tag{1.10}$$

where ρ is the total density of the liquid and E_{ph} the energy of the phonon gas which is proportional to T^4.

One can evaluate the effective roton mass density ρ_{r} in a similar way. Having found ρ_{r} and ρ_{ph} one has determined the normal fluid density,

$$\rho_{\text{n}} = \rho_{\text{r}} + \rho_{\text{ph}}, \tag{1.11}$$

as well as the superfluid density

$$\rho_{\text{s}} = \rho - \rho_{\text{n}}. \tag{1.12}$$

Landau suggests that the λ-point can be defined as that for which the temperature is such that $\rho_n = \rho_s$.

The basic idea of Landau is thus that the equilibrium properties of He II can be expressed as a gas consisting of (non-interacting) phonons and rotons, and is based on the fact that the only system statistical mechanics can deal with satisfactorily is a perfect gas. In other words, for sufficiently low temperatures one may assume that the excitation of the liquid helium can be considered to be a gas of phonons and rotons and, moreover, a perfect gas of these elementary excitations.

Let us now consider the question of superfluidity at absolute zero temperature. One must show that when helium flows through a capillary at a constant velocity $\vec{V}$ it cannot be slowed down by exciting an elementary excitation, provided $\vec{V}$ is smaller than some critical velocity. In order to see this, let us find the energy necessary to create an excitation of momentum $\vec{p}$. Suppose a body of velocity $\vec{V}$ and mass M creates an excitation and ends up moving with velocity $\vec{V}'$. From momentum conservation

$$M\vec{V} = M\vec{V}' + \vec{p}, \tag{1.13}$$

so that the new kinetic energy of the body is

$$\frac{1}{2M}(MV')^2 = \frac{M}{2}V'^2 = \frac{1}{2M}(M\vec{V} - \vec{p})^2 = \frac{1}{2}MV^2 - \vec{V}\cdot\vec{p} + \frac{p^2}{2M}. \tag{1.14}$$

If $\varepsilon(\vec{p})$ is the energy of an elementary excitation of momentum $\vec{p}$, this excitation cannot be created unless

$$\frac{1}{2}MV^2 \geq \frac{1}{2}MV'^2 + \varepsilon(\vec{p}). \tag{1.15}$$

Consequently

$$\varepsilon(p) \leq \frac{1}{2}MV^2 - \frac{1}{2}MV'^2 = \vec{V}\cdot\vec{p} - \frac{p^2}{2M}. \tag{1.16}$$

For large M, $\varepsilon(p) \leq \vec{V}\cdot\vec{p}$. Thus, the critical velocity necessary to create an elementary excitation in He II is then derived by drawing a tangent to the dispersion relation $\varepsilon(p)$ versus p (see Fig. 1.6), i.e.

$$V_c = \frac{\varepsilon(p)}{p}. \tag{1.17}$$

There are two solutions of this relation. One occurs at the origin,

$$(V_c)_{\text{phon}} = c_s, \tag{1.18}$$

which indicates that the critical velocity for the creation of phonons is the velocity of first sound (239 m s^{-1}).

To find the second solution of (1.16), one draws the straight line which passes through the origin and touches the curve close to the roton minimum. This leads to

$$(V_\mathrm{c})_\mathrm{rot} \approx \frac{\Delta}{p_0} = 58\,\mathrm{m\,s^{-1}}. \tag{1.19}$$

Because $(V_\mathrm{c})_\mathrm{rot} < (V_\mathrm{c})_\mathrm{phon}$, $(V_\mathrm{c})_\mathrm{rot}$ is the critical velocity for superfluidity.

Note also that the condition given in equation (1.17) for the case of the free-particle parabola (see Fig. 1.6) is

$$(V_\mathrm{c})_\mathrm{sp} = 0. \tag{1.20}$$

A critical velocity of zero means that superfluidity is impossible in any system where free-particle motion can take place. Thus, it is the energy gap Δ, together with the lack of any other thermal excitation below the dispersion relation shown in Fig. 1.6, which ensures a finite value of the critical velocity in He II. Detailed calculations of the dispersion relations shown in Fig. 1.6 have been carried out starting from the classical papers of Feynman (1972), see also Belyaev (1958a, 1958b), Hugenholtz and Pines (1959), Brueckner and Sawada (1957a, 1957b), Alberico *et al*. (1976) and references therein.

1.5 Critical velocity for superconductors

The excitation spectrum of a superconducting metal worked out by Bardeen, Cooper and Schrieffer (Bardeen *et al*., 1957a,b; Chapter 3) is shown in Fig. 1.7.

The Landau criterion for superconductivity gives the critical velocity

$$(V_\mathrm{c})_\mathrm{sc} = \frac{\Delta}{\hbar k_\mathrm{F}}. \tag{1.21}$$

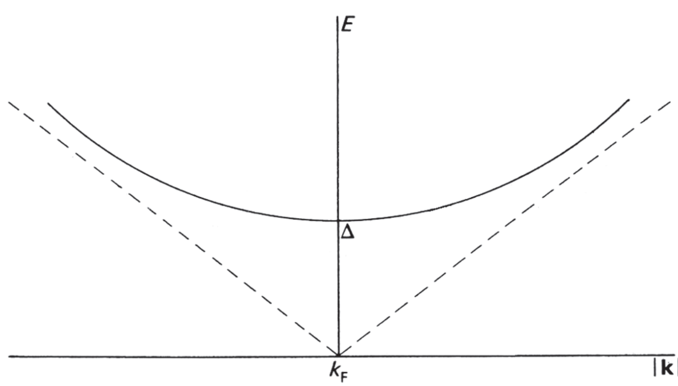

Figure 1.7. Sketch of the BCS excitation spectrum (full line) $E_k = \sqrt{(\varepsilon_k^2 + \Delta^2)}$, with the normal spectrum $|\varepsilon_k|$ (broken line). The normal spectrum is $\varepsilon_k = \hbar^2 k^2/2m_e - \hbar^2 k_\mathrm{F}^2/2m_e$ which can be approximated by $\varepsilon_k = \nu'_\mathrm{F}(|k| - k_\mathrm{F})$ with $\nu'_\mathrm{F} = \hbar k_\mathrm{F}/m_e$.

https://doi.org/10.1017/9781009401920.002 Published online by Cambridge University Press

Using the values for Sn

$$k_{\mathrm{F}} = 1.64 \times 10^{8}\ \mathrm{cm}^{-1}, \tag{1.22}$$
$$T_{\mathrm{c}} = 3.72\,\mathrm{K} = 0.32\ \mathrm{meV}, \tag{1.23}$$

and the BCS relation (Section 1.7)

$$\frac{2\Delta(0)}{T_{\mathrm{c}}} = 3.5, \tag{1.24}$$

one obtains

$$(V_{\mathrm{c}})_{\mathrm{sc}} = \frac{\Delta}{\hbar k_{\mathrm{F}}} = 51.2\ \mathrm{m\,s}^{-1} \tag{1.25}$$

where use was made of $\hbar c \approx 2 \times 10^{-2}$ meV cm and $c = 3 \times 10^{8}\ \mathrm{m\,s}^{-1}$. For the case of nuclei see Appendix K.

The use of Δ for both the (BCS) superconducting energy gap (see Fig. 1.7) and the roton energy minimum in neutral superfluids (see Fig. 1.6) is so well established in the literature that it is preferable to retain this double usage, at the risk (hopefully slight) of confusion.

1.6 Pairing in nuclei

The shell model potential is the average potential for a nucleon moving in a nucleus. It has a central and a spin-orbit component and, in a spherical nucleus, the individual nucleon states are specified by an orbital angular momentum l, a total angular momentum $j(= l \pm \frac{1}{2})$ and an eigenvalue m of j_z (Brink and Satchler, 1968). The nucleons interact through a strong, short-range, attractive nuclear force which contributes both to the shell model potential and to the residual interaction between nucleons. Two neutrons (or two protons) can best take advantage of the residual interaction to minimize their energy by moving in time-reversed orbits, i.e. states with the same j but equal and opposite m. The residual interaction (being time-reversal invariant) preserves the time-reversed motion because when such a pair of nucleons interact they scatter into time-reversed states. The total angular momentum of the pair is zero.

The ground state of a nucleus with an even number of neutrons and protons is obtained by coupling like nucleons in states with energies near the Fermi energy to form zero angular momentum pairs. Excited states are formed by breaking pairs, and the lowest states are constructed by breaking one pair. These states have an excitation energy of about 2Δ which is the pair binding energy (see Fig. 1.8).

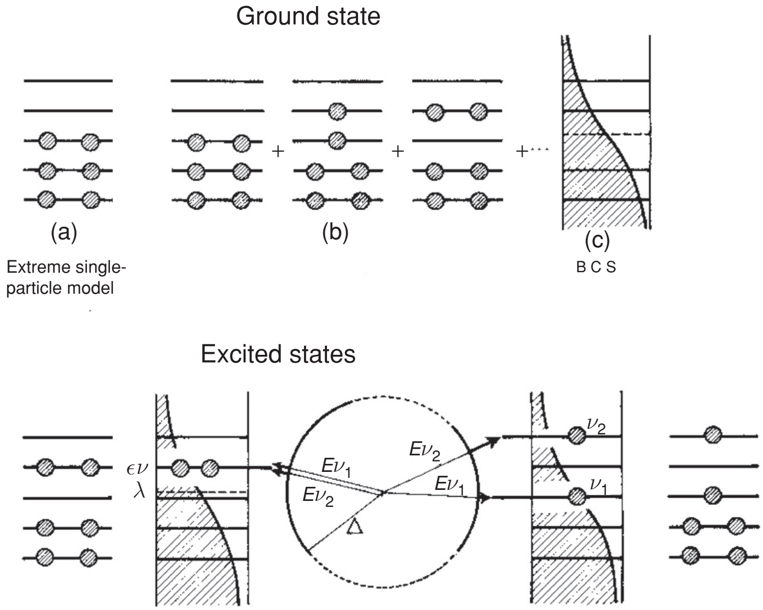

Figure 1.8. Schematic picture of the ground state and of the lowest excited states with angular momentum zero and positive parity in a system with an even number of fermions moving in a set of single-particle levels, assumed to be double degenerate.
Ground state: the ground state is obtained, in this extreme independent particle model, by filling the lowest orbitals compatible with the Pauli principle. The large energy gap observed in the nuclear spectrum is understood assuming a large energy loss not only to the breaking of a pair, but also to the lifting of pairs from one level to another; these two process are indicated in (b). That is, in the case where pairing correlations are taken into account, the ground state is a linear combination of pairs of particles in time-reversal states distributed over all the available levels. Thus the pair-correlated ground state consists of pairs scattering across the diffuse Fermi surface, a basic feature which is reflected in the occupation number shown to the far right (c).
Excited states: excited states can thus only be generated by breaking a pair of particles in any two levels, as shown in the lower part of the figure. Because the energy associated with each particle of the pair is $E_\nu = \sqrt{(\varepsilon_\nu - \lambda)^2 + \Delta^2}$, where ε_ν is the single-particle energy, λ is the Fermi energy and Δ the pairing gap, the minimum excitation energy is 2Δ, as shown. Note that the radius of the circle is the pairing gap, which measures the diffusivity of the Fermi surface. To the far left and right we show the extreme single-particle configurations associated with the two quasiparticle states shown close to the pairing gap circle, as well as the two-particle and two-quasiparticle excitation energy (after Nathan and Nilsson (1965)). Reprinted from *Alpha- Beta- and Gamma-Ray Spectroscopy*, Vol. 1, Nathan, H. and Nilsson, S. G., Editor Siegbahn, H., page 601, Copyright 1965, with permission from Elsevier.

The odd nucleon in a nucleus with an odd number of neutrons or protons must remain unpaired. One can obtain a qualitative description of the low states of such a nucleus in terms of the orbits available to the unpaired nucleon. In this approximation the degrees of freedom of the paired nucleons are neglected.

https://doi.org/10.1017/9781009401920.002 Published online by Cambridge University Press

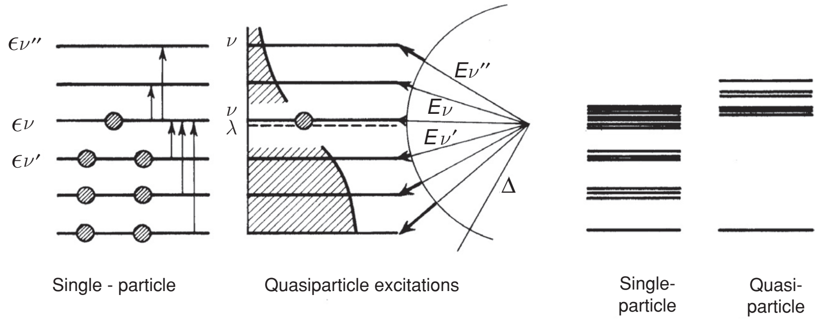

Figure 1.9. Ground state and excited states in the extreme independent single-particle model and in the pairing-correlated, superfluid model in the case of a system with an odd number of particles. In the first case, the energy of the ground state of the odd system differs from that of the even with one particle fewer by the energy difference $\varepsilon_\nu - \varepsilon_{\nu'}$, while in the second case by the energy $E_\nu = \sqrt{(\varepsilon_\nu - \lambda)^2 + \Delta^2} \approx \Delta$, associated with the fact the odd particle has no partner. Excited states can be obtained in the independent particle case by promoting the odd particle to states above the level ε_ν, or by exciting one particle from the state below to the state ε_ν or to one above it. To the left only a selected number of these excitations are shown. In the superfluid case excited states can be obtained by breaking of pairs in any orbit. The associated quasiparticle energy is drawn also here by an arrow of which the thin part indicates the contribution of the pairing gap and the thick part indicates the kinetic energy contribution, i.e. the contribution arising from the single-particle motion. Note the very different density of levels emerging from these two pictures, which are shown at the far left of the figure (after Nathan and Nilsson (1965)). Reprinted from *Alpha- Beta- and Gamma-Ray Spectroscopy*, Vol. 1, Nathan, H. and Nilsson, S. G., Editor Siegbahn, H., page 601, Copyright 1965, with permission from Elsevier.

When pairing correlations are taken into account this system in its ground state has an excitation energy of the order of Δ compared with the even system (see Fig. 1.9).

This effect leads to an odd–even staggering in nuclear masses and nucleon separation energies. If $B(N, Z)$ is the binding energy of a nucleus with Z protons and N neutrons then the energy required to separate the last neutron is

$$S_n(N, Z) = B(N, Z) - B(N - 1, Z). \tag{1.26}$$

Similarly the separation energy for the last proton is

$$S_p(N, Z) = B(N, Z) - B(N, Z - 1). \tag{1.27}$$

On average the neutron separation energy $S_n(N, Z)$ should be larger for a nucleus with even N compared with a nucleus with odd N by the neutron pairing energy 2Δ. Fig. 1.10 shows the neutron separation energy for a sequence of nuclei

https://doi.org/10.1017/9781009401920.002 Published online by Cambridge University Press

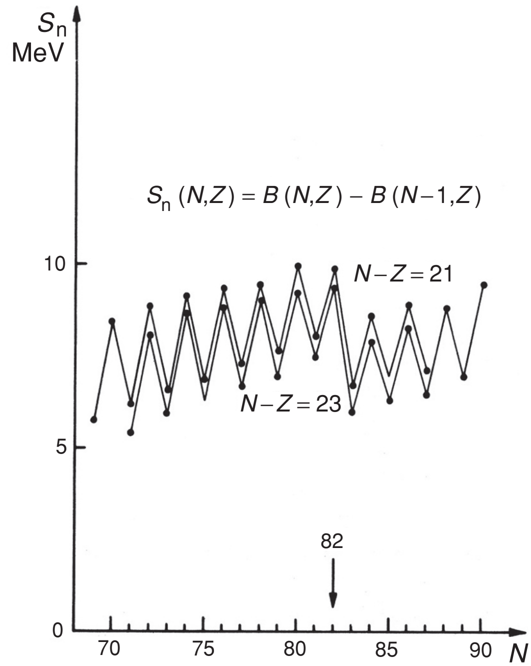

Figure 1.10. The neutron separation energies, S_n, are taken from the compilation by J. H. E. Mattauch, W. Thiele and A. H. Wapstra, Nuclear Phys. **67**, 1 (1965) (after Bohr and Mottelson (1969)).

with $N - Z = 21, 23$, i.e. in the neighbourhood of the $N = 82$ closed shell. There is a general tendency for S_n to increase as N increases but super-imposed on this trend there is a clear odd–even staggering effect due to pairing.

Values for the neutron pairing energy, known as the pairing gap, can be obtained from measured separation energies by using the formula

$$\begin{aligned}\Delta_n &= \tfrac{1}{4}\{2S_n(N, Z) - S_n(N+1, Z) - S_n(N-1, Z)\}\\ &= \tfrac{1}{4}\{B(N-2, Z) - 3B(N-1, Z) + 3B(N, Z) - B(N+1, Z)\}\,,\end{aligned} \tag{1.28}$$

where N is even. Similarly, the proton separation energy is given by

$$\begin{aligned}\Delta_p &= \tfrac{1}{4}\big\{2S_p(N, Z) - S_p(N, Z+1) - S_p(N, Z-1)\big\}\\ &= \tfrac{1}{4}\{B(N, Z-2) - 3B(N, Z-1) + 3B(N, Z) - B(N, Z+1)\}.\end{aligned} \tag{1.29}$$

Empirical values of the pairing energy parameters Δ_n and Δ_p are collected in Fig. 1.11. The general trend with mass number A can be fitted by the formula

https://doi.org/10.1017/9781009401920.002 Published online by Cambridge University Press

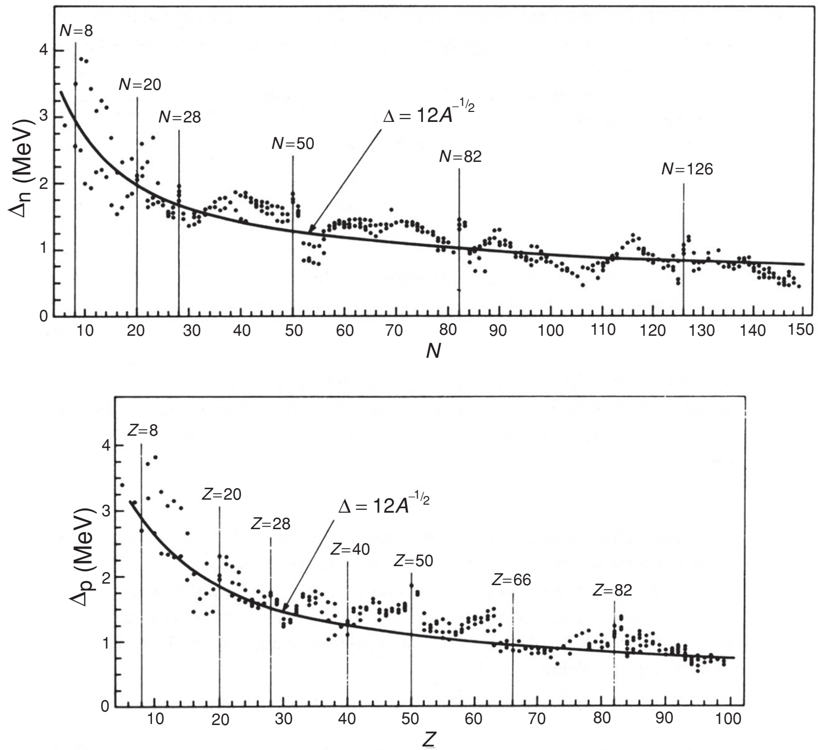

Figure 1.11. The odd–even mass differences for neutrons and protons are based on the analysis of Zeldes *et al*. (1967) (after Bohr and Mottelson (1969)).

(see Bohr and Mottelson (1969)).

$$\Delta \approx 12/A^{\frac{1}{2}} \text{ MeV}. \tag{1.30}$$

Conspicuous local variations of the pairing gap with the number of neutrons or protons are observed, which cannot be fitted in detail by the smooth behaviour given by expression (1.30) (see e.g. Fig. 10.6). This A-dependence of Δ correlates, as a rule, with the collectivity displayed by low-lying surface vibrations of the different isotopes or isotones (see e.g. Fig. 10.7). This correlation testifies to the fact that, in addition to the bare nucleon–nucleon force, the exchange of collective surface vibrations between nucleons moving in time-reversal states close to the Fermi energy contributes to nuclear pairing correlations. The relative importance of this induced pairing interaction compared with the bare nucleon–nucleon interaction is a subject which is discussed in Chapters 8, 9, 10 and 11.

1.7 Superconductivity

Electrons near the Fermi surface in a superconductor interact to form correlated pairs. This idea was first suggested by Cooper (1956) and the pairs are often called 'Cooper pairs'. Cooper pairs are constructed from states in which the two electrons have zero total spin and equal and opposite linear momentum **k** and −**k**. The interaction which produces pairing correlations in a normal superconductor is a coupling between electrons via the positive ions of the crystal lattice. The electrons are coupled to the lattice by electrostatic forces. An electron moving through a crystal distorts the lattice and this distortion influences the motion of other electrons. Another way of expressing this is to say that an electron can emit or absorb a virtual phonon. The effective interaction between electrons is a result of the virtual emission of a phonon by one electron and its absorption by another. This interaction causes scattering of an electron pair from states ($\mathbf{k}, -\mathbf{k}$) to states ($\mathbf{k}', -\mathbf{k}'$) with an amplitude $V_{\mathbf{k}'\mathbf{k}}$ which depends on the electron–phonon coupling and on the phonon spectrum (see Fig. 1.12).

The interaction which produces pairing correlations in a normal superconductor is the result of a delicate balance between Coulomb repulsion screened by dynamical polarization effects of both electrons (plasmons) and ions (phonons). The screening of the Coulomb repulsion due to the exchange of plasmons (measured by the dimensionless parameter $\mu*$) plays an equally important role in determining the properties of superconductors as the effective interaction arising from the exchange of phonons (measured by the dimensionless parameter λ). Systems displaying small ($\ll 1$) values of $\mu*$ and large ($\gtrsim 0.3 - 0.4$) values of λ are expected to be normal or incipient high-T_c superconductors, such as

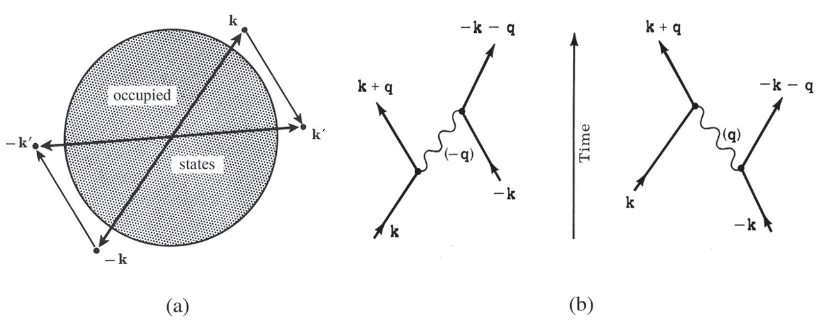

Figure 1.12. Schematic representation of the Cooper pair phenomenon. In (a) a transition is illustrated in which one pair of electrons moving in time-reversal states above the Fermi sea and carrying zero centre-of-mass momentum interact, exchanging momentum $\vec{q}$. The carriers of this interaction are the lattice phonons which are exchanged between the two electrons, as shown in (b).

https://doi.org/10.1017/9781009401920.002 Published online by Cambridge University Press

alkaline doped fullerides, i.e. materials made out of e.g. C_{60} fullerenes, in which case $\mu* \approx 0.3$ and $\lambda \approx 1$ (Gunnarsson (1997), (2004), Broglia *et al.* (2004)).

In the nuclear case the situation is quite different, as the strong force is (for relative distances $\gtrsim 0.75$ fm) attractive in the s-wave channel (see Figs. 8.2 and 8.5). Consequently, the main origin of nuclear pairing is due to the nucleon–nucleon strong force.

It is found, however, that the exchange of collective surface vibrations between pairs of nucleons moving in time-reversal states lying close to the Fermi energy seems to play a role which cannot be neglected in a quantitative description of pairing in nuclei (Chapters 8, 9, 10 and 11). The main differences between the phonon exchange in solids and in nuclei is that nuclear vibrations can be viewed as coherent motion of nucleons. To take care of Pauli principle violations as well as to avoid double counting of the same degrees of freedom, nuclear field theoretical methods have to be used in the calculation of the coupling of nucleons to nuclear surface vibrations leading to an induced pairing interaction (see Bes *et al.* (1976a,b), Bortignon *et al.* (1977), see also Appendix F).

Returning now to the case of superconductors, each Cooper pair has a binding energy 2Δ which is much smaller than the Fermi energy ε_F. The main components of the pair wavefunction come from electron states with energies ε within Δ of the Fermi energy,

$$\varepsilon_F - \Delta < \varepsilon < \varepsilon_F + \Delta. \tag{1.31}$$

The energy spread $\delta\varepsilon \approx 2\Delta$ corresponds to a momentum range $\delta p \approx 2\Delta/v_F$ where v_F is the Fermi velocity. The uncertainty relation $\delta x \approx \hbar/\delta p \approx \hbar v_F/2\Delta$ gives an estimate of the size of a Cooper pair. The quantity

$$\xi = \frac{\hbar v_F}{2\Delta} \tag{1.32}$$

is called the coherence length or correlation length of the superconductor, and is a measure of the size of a Cooper pair. The coherence length ξ is much larger than the crystal lattice spacing ($\sim$5 Å) in Type I superconductors. The Fermi velocity of electrons in these materials is normally large ($v_F \approx 10^6$ m s^{-1}) and the energy gap is small, leading to a large coherence length. For example $\xi \approx 10714$ Å for Sn and $\xi \approx 4615$ Å for Pb. Type II superconductors have a much smaller coherence length ($\xi \approx 50$ Å). This is partly because the electrons in these materials have a large effective mass and a small Fermi velocity ($v_F \approx 10^4$ m s^{-1}). Also, the energy gap is usually larger.

Bardeen, Cooper and Schrieffer (1957a,b) and Schrieffer (1964) developed a microscopic theory of superconductivity which incorporated the idea of Cooper pairs and gave a consistent treatment of the Pauli principle. The theory (called the BCS theory) has also been used to describe pairing in nuclei (Bohr, Mottelson and Pines (1958)) and is discussed in Chapter 3 of this book. According to the BCS theory all electrons near the Fermi surface in the ground state of a superconductor form correlated Cooper pairs. Excited states are formed by breaking pairs and there is an energy gap 2Δ between the ground state and the lower excited states (Fig. 1.8). It is this energy gap which stabilizes the superconducting state. Thermal effects can break pairs, and in BCS theory the presence of unpaired electrons reduces the binding of those pairs which remain. Thus the gap parameter 2Δ is temperature dependent and decreases as T increases. At a critical temperature T_c the energy gap becomes zero, the pairs are broken and there is a phase transition from the superconducting phase into the normal phase. BCS theory predicts a definite relation between the transition temperature T_c and the energy gap $\Delta(0)$ at $T = 0$, namely,

$$\frac{2\Delta(0)}{T_c} = 3.51. \tag{1.33}$$

This relation can be checked experimentally because both $\Delta(0)$ and T_c can be measured. For most normal superconductors the ratio lies in the range 3.2–4.6 and is close to the BCS value.

These concepts have had also a profound influence on the theory of elementary particles. The Nambu–Jona-Lasinio model (1961a,b) was the first to pursue such matters, assuming that a kind of superconducting material occupied the whole Universe. This corresponds to the Higgs field introduced in later developments. In this world, particles and antiparticles, e.g. quarks and antiquarks, are the constituents of the Cooper pairs. Breaking one of these pairs produces a massive quark and a massive antiquark. Disturbing the distribution of the pairs creates waves (Anderson–Nambu–Goldstone modes) which can be interpreted as bosons, e.g. pions (see Chapter 4). The role which gauge invariance (charge conservation) plays in the BCS theory is played here by chiral invariance (invariance with respect to left-handedness and right-handedness operations).

Leggett (1989) points out that the Cooper pairs in the BCS theory of the superconducting state must all behave in exactly the same way, not only as regards their internal structure but also as regards their centre of mass motion. Each Cooper pair is made up of two fermions and therefore the pairs behave like bosons. From this point of view superconductivity is due to Bose condensation of the pairs. The analogy is not complete. In a Bose liquid such as ^{4}He the bosons exist even when they are not all condensed, while in the superconducting state either the Cooper pairs are condensed or they do not exist. Such a picture should, however, be modified for finite systems like nuclei, as well as for superconductors around the critical temperature and for superconducting metal clusters (see Section 1.9). In the nucleus, pairing vibrations (Chapter 5), i.e. collective modes which change the number of pairs, play an important role. They can be viewed as bound states

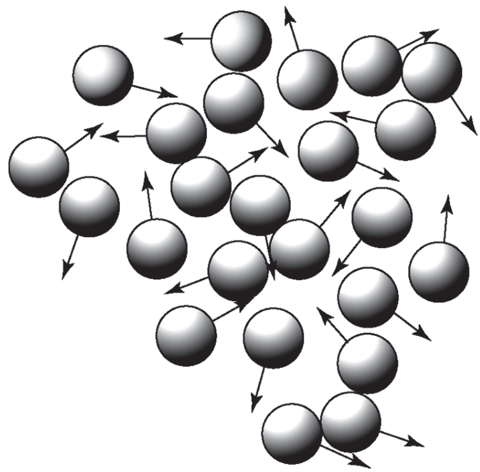

Figure 1.13. A system of independent Cooper pairs (Schafroth pairs). This situation corresponds to the incoherent solution of the many Cooper pair problem, the so called Fock state.

at the top of the Fermi surface (Anderson (1958), Högaasen-Feldman (1961), Bes and Broglia (1966)). In finite systems the presence of incipient Cooper pairs smooths out the sharp phase transition predicted by BCS theory.

There is another important fact to be considered in connection with the description of superconductors in terms of electron pairs. As pointed out by Schrieffer (1964) the pairs could be treated as independent if they were well separated (see Fig. 1.13), and Cooper's discussion would be appropriate for Schafroth (1955) pairs, see also Ogg (1946), Blatt and Butler (1955); note also the renewed interest in Schafroth pairs in connection with high T_c superconductivity (Alexandrov, 2003). However, actual superconductors differ in a fundamental manner from a bound-pair model in which the pairs are well separated in space and weakly interacting. The pairs overlap strongly and there are, in a superconducting metal, on average one million bound pairs (eliminating electrons deep in the Fermi sea) which have their centres of mass falling within the region occupied by a given pair wavefunction (see Fig. 1.14).

The study of Bose–Einstein condensation (BEC) has opened new interest on the study of the two, widely different, regimes schematically depicted in Figs. 1.13 and 1.14. In particular, with the possibility of studying ultracold Fermi gases of, for example, alkali metal atoms (Jochim *et al.* (2003), Greiner *et al.* (2003), Zwierlein *et al.* (2003), Regal *et al.* (2004)) like potassium or lithium, whose nucleus has an even integer spin but an odd number of protons and of neutrons ($^{40}_{19}K_{21}$, $^{6}_{3}Li_3$). A notable property of these atomic gases is the presence of scattering resonances, so called Feshbach resonances. A Feshbach resonance is an enhancement in the scattering amplitude of a particle incident on a

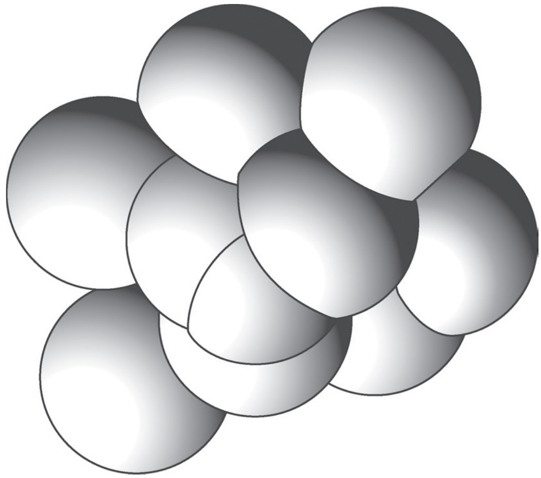

Figure 1.14. There are about 10^{18} Cooper pairs per cm^3 in a superconducting metal. A Cooper pair has a spatial extension of about 10^{-4} cm. Thus a given Cooper pair will overlap with 10^6 other Cooper pairs, leading to strong pair–pair correlation, as schematically shown. This solution corresponds to the coherent solution of the many Cooper pair problem (coherent state).

target – for instance, a nucleon scattering from a nucleus or an atom scattering from another atom – when it has approximately the energy needed to create a quasi-bound state of the two-particle system.

If a pair of ultracold atoms happens to have a bound state (molecular state) close to zero energy, then during collisions they will stick together for a while as they undergo a Feshbach resonance. While few molecules have a bound state near zero energy, Feshbach resonances can be produced using an external magnetic field (Zeeman tuning). The resonance is induced in the scattering between two atoms in different internal states, typical hyperfine states, and results in the divergence in the two-body s-wave scattering length α_F (the interaction between a pair of ultracold atoms is directly proportional to α_F). Feshbach resonances allow the experimental study of a Fermi gas at various interaction regimes. By varying the value of α_F (atoms repel if α_F is positive and attract if it is negative), one can explore different kinds of fermionic superfluidity, ranging from the BCS superfluidity, to BEC. Momentum correlations in Cooper-paired particles extend over long distances, whereas correlations in a molecule are short range. Consequently, the diatomic molecules do not constitute Cooper pairs. However, the molecules can be dissociated by moving the system back across the Feshbach resonance into the atomic regime. Interest in the transition from BEC-like behaviour to BCS-like behaviour was discussed, even before the discovery of Bose–Einstein condensation, by Leggett (1980).

Superconductors have unusual magnetic properties. When a sample of superconductor is placed in a magnetic field supercurrents are developed inside it which exclude the magnetic flux. Type I superconductors exclude the magnetic flux B completely for applied fields H less than a critical field H_c. This is the Meissner effect (Meissner and Ochsenfeld (1933)). Above H_c there is complete flux penetration and the normal state is restored. The Meissner effect is more complicated in a Type II superconductor in that there are two critical fields $H_{c1} < H_{c2}$. There is complete exclusion of flux if $H < H_{c1}$ and partial penetration for $H_{c1} < H < H_{c2}$ The critical field H_{c2} depends on temperature and goes to zero at the critical temperature T_c. Magnetic fields reduce or destroy superconductivity because they break time reversal invariance and reduce the binding of the Cooper pairs. When discussing magnetic effects it is important to make a distinction between the fields H and B. A number of conventions are possible depending on whether the supercurrent is regarded as an external current or a magnetization current. One convention which is commonly used is that H is generated by external currents and is unaffected by the presence of the superconductor. Supercurrents are considered to be magnetization currents which modify the flux B, but do not affect H.

The Ginzburg–Landau (1950) theory is a phenomenological theory of superconductivity which is based on Landau's theory of second order phase transitions (see e.g. Patashinskii and Pokrovskiĭ (1979) and refs. therein). Landau had argued that such a transition is characterized by an order parameter in a simple way. Ginzburg and Landau applied the method to superconductors. They introduced a complex order parameter ψ which could be interpreted as a kind of macroscopic wavefunction for the superconductor. In the presence of a magnetic field the free energy density is

$$f(\mathbf{r}) = f_0 + \alpha|\psi(r)|^2 + \frac{1}{2}\beta|\psi(r)|^4 + \frac{1}{2m^*}|(-\mathrm{i}\hbar\vec{\nabla}\psi - q\mathbf{A}\psi)|^2 + \frac{1}{2}\mu_0\mathbf{B}^2. \tag{1.34}$$

Here $\mathbf{A}$ is the vector potential of the magnetic field $\mathbf{B}$, q is the charge of the carriers of the supercurrent, and α and β are temperature-dependent constants. The Ginzburg–Landau theory is gauge-invariant provided that a gauge transformation of the vector potential is associated with a change in the phase of the order parameter. One can check that the gauge transformation

$$\psi' = \mathrm{e}^{\mathrm{i}\chi}, \quad \mathbf{A}' = \mathbf{A} + \hbar\vec{\nabla}\chi/q \tag{1.35}$$

leaves the free energy invariant. The electric current density is (see also Section 1.2)

$$\mathbf{J}(\mathbf{r}) = \frac{q\hbar}{2m^*\mathrm{i}}(\psi^*\vec{\nabla}\psi - \psi\vec{\nabla}\psi^* - 2\mathrm{i}q\mathbf{A}\psi^*\psi/\hbar), \tag{1.36}$$

https://doi.org/10.1017/9781009401920.002 Published online by Cambridge University Press

and is also invariant with respect to the gauge transformation given in equation (1.35). The quantity m^* is the effective mass of the carriers. The Ginzburg–Landau theory gives a good description of the magnetic properties of both Type I and Type II superconductors and predicts that magnetic flux is quantized in certain situations.

The magnetic flux trapped in a superconducting ring is quantized and the quantization condition can be derived from the form (1.36) of the supercurrent and the condition that the order parameter is single valued. There may be supercurrents in the surface of a ring enclosing magnetic flux but the current in the interior is zero. Also, the magnitude of the order parameter will be approximately constant in the interior of the material of the ring. If we write $\psi = |\psi| \exp(\mathrm{i}\phi)$ then the condition that the current density (1.36) is zero gives

$$\hbar \nabla \phi - q\mathbf{A} = 0. \tag{1.37}$$

If ψ is single valued then ϕ can be changed by an integer multiple of 2π around the ring. Integrating equation (1.37) along a path C inside the ring gives the flux quantization condition

$$\Phi = \oint_C \mathbf{A} \cdot \mathbf{dl} = n2\pi\hbar/q \tag{1.38}$$

where n is an integer.

The quantum $2\pi\hbar/q$ of magnetic flux has been measured (Parks and Little (1964)) with the result that the charge of the carriers of the supercurrent is $|q| = 2e$, that is e^* (Section 1.2). This result indicates that the carriers of the supercurrent are the Cooper pairs of the BCS theory. The absence of electrical resistance in a superconductor is due to the binding energy 2Δ of the pairs. Because of this binding the electrons cannot scatter individually (note, however, the discussion at the end of Section 1.2).

The BCS theory describes a superconductor in equilibrium. An extension to include departures from equilibrium using the time-dependent mean-field approximation was made by Gor′kov (1960a,b) who established a connection between the BCS microscopic theory and the phenomenological Ginzburg–Landau theory. Gor′kov introduces a pair-field $\Delta(\mathbf{r})$ which in general is complex and position-dependent. In an equilibrium situation $2\Delta(\mathbf{r})$ is the BCS energy gap between the ground state and excited states. Gor′kov showed that the pair field $\Delta(\mathbf{r})$ is essentially the same as the order parameter $\psi(\mathbf{r})$ of the Ginzburg–Landau theory except for a constant factor due to the different normalization of ψ (see also Bes *et al*. (1970)).

1.8 Superfluidity of liquid ^{3}He

When the effective interaction $V_{\mathbf{k},\mathbf{k}'}$ for scattering of an electron pair from a state $(\mathbf{k}, -\mathbf{k})$ to a state $(\mathbf{k}', -\mathbf{k}')$ is independent of the angle between $\mathbf{k}$ and $\mathbf{k}'$

then the Cooper pairs have zero orbital angular momentum and the pairing is called s-wave pairing. The Pauli principle requires that the pair wavefunction should be antisymmetric. As the orbital state is symmetric, the spin state must be antisymmetric and the pair must be in singlet state with spin $S = 0$. Most superconductors have s-wave pairing, but there could be a component of d-wave pairing due to crystal field effects. Pairing in nuclei is essentially s-wave pairing, although there is also evidence for d-wave pairing (Section 5.3 and Section 6.2.2). Furthermore, because of the presence of two types of fermions (protons and neutrons), the isospin dependence of pairing is important in nuclei (Bohr (1968), Nathan (1968), Bayman *et al*. (1969), Bes *et al*. (1977)).

The situation is different in the superfluid state of liquid ^{3}He because the interaction potential between ^{3}He atoms is strongly repulsive at small separations. This repulsion inhibits s-wave pairing and favours pairs with non-zero orbital angular momentum. Experimental and theoretical work has shown that p-wave pairing is important. In this case the orbital wave function of a pair of ^{3}He atoms is antisymmetric. Then the Pauli principle requires the spin of the pair to be symmetric with $S = 1$ and there is spin triplet pairing.

Triplet pairing is more complicated than singlet pairing. A pair has spin angular momentum $S = 1$ and orbital angular momentum $L = 1$ and there are several ways in which S and L can couple. The Ginzburg–Landau order parameter has nine complex components. It is for this reason that the superfluid phases of ^{3}He have a very rich structure. There are many superfluid phases. Two of them are the A-phase and the B-phase. In the A-phase the spin part of the wavefunctions is $|\uparrow\uparrow\rangle$ or $|\downarrow\downarrow\rangle$ while in the B-phase the pairing includes the combination $|\uparrow\downarrow\rangle + |\downarrow\uparrow\rangle$. The structure of the phases is anisotropic on a small scale due to various spin alignment correlations (see Vollhardt and Wölfle (1990) and refs. therein). The phase structure of ^{3}He was predicted by Leggett (1972) see also Anderson and Morel (1961), Balian and Werthamer (1963), Anderson and Brinkman (1973), (1975) and Ambegaokar and Mermin (1973)).

1.9 Comparison of pairing in nuclei with superconductivity

In this section we point out some of the differences between pairing properties of nuclei and superconductors. The coherence length in a superconductor is defined in equation (1.32). It measures the size of a Cooper pair. In both Type I and Type II superconductors the coherence length is large compared with the interatomic spacing in the material but small compared with the typical size of a piece of superconducting material. The situation is very different in a nucleus. Using the appropriate Fermi wave number ($k_{\mathrm{F}} \approx 1.36\,\mathrm{fm}^{-1}$) we get $\hbar\upsilon_{\mathrm{F}} = 54\,\mathrm{MeV}$ fm. Then equation (1.32) gives a coherence length

$$\xi \approx \frac{27}{\Delta}\,\mathrm{fm}, \tag{1.39}$$

https://doi.org/10.1017/9781009401920.002 Published online by Cambridge University Press

the gap being in units of MeV. For a typical nucleus with $A = 140$, $\Delta \approx 1$ MeV, $\xi \approx 27$ fm. This compares with a nuclear radius $R = 1.2A^{1/3}$ fm ≈ 6.3 fm for medium heavy nuclei ($A \approx 120$). Thus the coherence length is larger than the nuclear radius. The same result holds for all nuclei in the periodic table. In a nucleus the size of a Cooper pair is given by the nuclear size rather than by the coherence length.

Quantum size effects can modify the properties of a superconductor if its dimensions are small enough. The first changes occur when the size is small compared with the coherence length but is still large in comparison with interatomic distances. In principle such a superconductor has the same properties as a bulk sample so long as it is not in a magnetic field. The behaviour in a strong field has interesting features. For example, the energy gap in the energy spectrum disappears at a certain value of the field. However, this field is not yet strong enough to break the Cooper pairs, and other properties of the superconducting state are retained. When the field is increased further there is a second-order phase transition to the normal state. These and other properties of small superconducting particles have been reviewed by Perenboom *et al*. (1981) (see also Kubo (1962), Black *et al*. (1996), Ralph *et al*. (1997), Farine and Schuck (2002)).

Properties of a sample of a superconductor depend on its dimension. A two-dimensional film or a one-dimensional wire behave differently from a three-dimensional sample. The meaning of a thin film is that the thickness is small compared with the coherence length. Similarly, a wire is effectively one-dimensional if its radius is small compared with the coherence length. Using the same criteria a nucleus should be regarded as a zero-dimensional superconductor (Chapter 4).

If the dimensions of a superconducting particle become much smaller than the coherence length other effects come into play. Anderson (1959) suggested that there is a lower limit in size for a particle still to be superconducting. A relevant parameter for this regime is the ratio of the mean spacing of single particle states δ with the same spin to the transition temperature T_c

$$\bar{\delta} = \frac{\delta}{T_c} = \frac{2}{\rho(\varepsilon_F)T_c}, \tag{1.40}$$

where $\rho(\varepsilon_F)$ is the density of states at the Fermi level. Mühlschlegel *et al*. (1972) and Lauritzen *et al*. (1993) have calculated the effects of thermal fluctuations on the superconducting phase transitions using Ginzburg–Landau theory, path integral methods plus RPA theory, respectively. They show that the fluctuations smooth out the discontinuity in the thermal capacity at the transition temperature. The smoothing is complete when $\bar{\delta} = 1$, but is already significant if $\bar{\delta} \approx 0.01$. This smoothing has been observed experimentally by Tsuboi and Suzuki (1977). They measured the electronic specific heat of small particles of Sn with an average diameter ranging from 25 nm up to 220 nm. Some of their results are shown in Fig. 1.15.

https://doi.org/10.1017/9781009401920.002 Published online by Cambridge University Press

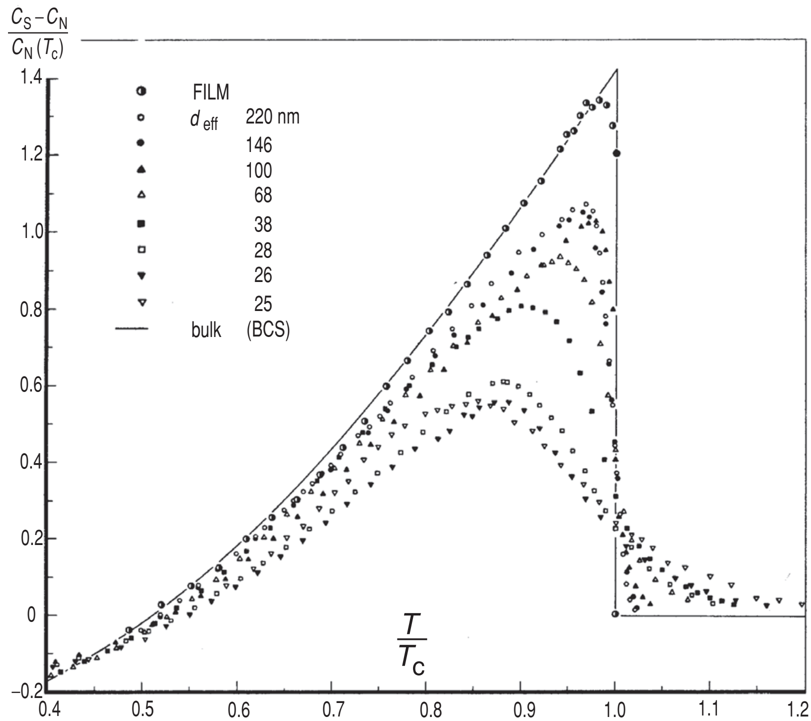

Figure 1.15. Measured normalized difference $(C_S - C_N)/C_N(T_c)$ of the specific heat in the superconductive and normal state respectively, for tin particles with different diameters, as a function of the reduced temperature. The measurements are normalized to $C_N(T_c) = \gamma T_c$, with $\gamma = 1.78 \times 10^{-3}\ \mathrm{JK^{-2}\ mol^{-1}}$. The ensemble of tin particles, isolated from each other by an oxide layer, was prepared by depositing tin islands in vacuum and then oxidising their surfaces repeatedly. From Tsuboi and Suzuki (1977).

Quantum size effects are also significant in nuclei and no sharp pairing phase transition is expected. Pairing correlations should definitely become weaker as the excitation energy is increased but there will be no sudden transition (Chapter 6).

Mottelson and Valatin (1960) argued that there is a close formal correspondence between the equations of motion in a constant magnetic field and those in a rotating reference system. They suggested that critical magnetic field phenomena in superconductors should have their counterpart in the rotational spectra of nuclei. The Coriolis forces in a rotating nucleus tend to decouple pairs of particles in time-reversal states. When the angular velocity is sufficiently large then pairing correlations should be destroyed completely. Mottelson and Valatin estimated a critical angular velocity ω_c above which there would no longer be any pairing correlation. This is analogous to the critical magnetic field B_c for a superconductor.

The correspondence between the effect of a magnetic field on a superconductor and the influence of rotations on pairing in a nucleus is not complete. The London penetration depth is destroyed by an applied magnetic field in two stages. In the absence of a magnetic field all the electrons are paired in the superconducting ground state. Excited states are formed by breaking pairs. The two-quasiparticle states have an excitation energy and so on. The magnetic field produces a Zeeman splitting of the excited states and reduces the energy gap. The splitting is largest in a quasiparticle state with maximum angular momentum. This is $k_F R$, where R is the radius of the particle and k_F is the Fermi momentum. When the field has a strength B_1 given by:

$$\frac{e\hbar}{2m}(2k_F R)B_1 = 2\Delta, \tag{1.41}$$

the lowest two-quasiparticle state becomes degenerate with the fully paired ground state. In these circumstances the field is strong enough to reduce the energy gap to zero but not strong enough to destroy the superconductivity. It is an example of gapless superconductivity (Perenboom *et al*. (1981)).

The two-quasiparticle state with highest angular momentum has a magnetic moment $(e\hbar/2m)2k_F R$, while the largest magnetic moment of a four-quasiparticle state is almost twice that value. Thus, when the field increases slightly above B_1, the four-quasiparticle state becomes degenerate with the fully paired state. As the field increases further, more and more pairs are broken. The resultant blocking reduces the effective strength of the pairing interaction and eventually the pairing disappears. Calculations reviewed in Perenboom *et al.* (1981) based on the BCS theory with a Fermi gas density of states and including no shell effects, give the critical field as

$$B_c = 2.6B_1. \tag{1.42}$$

The first of these size effects exists in rotating nuclei. As discussed in Brink (1994), the largest two-quasiparticle angular momentum is $j_1 + (j_1 - 1) = 2j_1 - 1$, where j_1 is the maximum single-particle angular momentum available near the Fermi level. Normally it corresponds to the intruder state with $j_{max} = l_{max} + 1/2$ which is pushed down from the next shell by the spin–orbit interaction. This two-quasiparticle state is split by the rotation and becomes degenerate with the fully paired state when

$$\hbar\omega_1 = \frac{2\Delta}{2j_1 - 1}. \tag{1.43}$$

Physically this size effect is associated with the band crossing (or ‘backbend’, see Chapter 6, Fig. 6.3) observed in rotating nuclei and ω_1 should be indentified with the band crossing frequency. The two quasiparticlcs align their angular momentum with the rotational axis of the nucleus.

Backbending is a striking effect which is observed in the rotational spectrum of many deformed nuclei. The corresponding effect is much more difficult to detect

https://doi.org/10.1017/9781009401920.002 Published online by Cambridge University Press

in superconductors because the critical field B_1 (see equation (1.41)) depends on the radius of the sample and it is difficult to obtain grains of uniform size. As well as producing backbending, rotations tend to quench the pair correlations in a nucleus. There should be a phase transition to an unpaired state at a critical rotational frequency ω_c. Analogy with the superconducting case equation (1.42) suggests $\omega_c \approx 2.6\omega_1$. Making use of equation (1.43) with typical values of $\Delta \approx 1.2\,\text{MeV}$ and $j_1 \approx 13/2$ for medium heavy nuclei ($A \approx 150$), leads to $\hbar\omega_c \approx 0.5\,\text{MeV}$.

As in the case of the critical temperature, finite size effects will smooth out any sudden phase transition. Pairing correlations should definitely be reduced as the angular velocity increases but they are unlikely to vanish suddenly at $\omega \approx \omega_c$.

Finite size effects in nuclei smooth out some of the striking effects associated with phase transitions in superconductors, but at the same time there are new phenomena associated with the finite size which are unknown in superconductors. Shell effects are a consequence of the finite size of nuclei. The spacing $\hbar w_0$ between major shells in a nucleus can be estimated from the formula (Bohr and Mottelson (1969))

$$\hbar w_0 \approx 41 A^{-1/3}\,\text{MeV} \approx \frac{49}{R}\,\text{MeV fm}, \tag{1.44}$$

where we have used $R = 1.2A^{1/3}$fm. Equations (1.39) and (1.44) give a relation

$$\frac{R}{\xi} \approx 1.8\frac{\Delta}{\hbar w_0}. \tag{1.45}$$

Thus the condition that the nuclear radius is small compared with the coherence length is related to a condition that the pairing strength 2Δ is less than the shell spacing $\hbar w_0$. Consequently, a phase transition from normal into superfluid states can take place at $T = 0$, as a function of particle number. In fact in closed shell nuclei $\Delta \ll \delta \approx 0.5\hbar w_0$ while in open shell nuclei $\Delta > \delta \approx \hbar w_0/10$. Spatial quantization in atomic nuclei leads to single-particle states with quite different angular momenta. Cooper pairs based on large angular momenta levels and lying close to the Fermi energy feel the action of nuclear rotation stronger than Cooper pairs based on low angular momenta levels. Consequently, the breaking of Cooper pairs takes place in atomic nuclei as a function of rotational frequency, stepwise. This interplay between pairing and shell effects is responsible for the band crossing or ‘backbending’ phenomena observed in rotating deformed nuclei (Stephens and Simon (1972), Bohr and Mottelson (1974, 1981), Broglia *et al.* (1974a), (1975)) (see Chapter 6).

1.10 Neutron stars

Atoms dissolve when ordinary matter is compressed to a very high density, namely when the separation of the nuclei is smaller than the atomic size. The positive charged nuclei move in a plasma of free electrons. For such an assembly the lowest energy state is reached for a system of $^{56}_{26}$Fe nuclei because they are the nuclei with the largest binding energy. If the matter is compressed to a still higher density the electron Fermi energy increases and the electrons become relativistic. For a sufficiently large density it becomes energetically favourable for the electrons to combine with the bound nuclear protons to form neutrons by inverse β-decay. This moves the equilibrium nuclear composition away from $^{56}_{26}$Fe to more neutron-rich nuclei. Coulomb forces play a weaker role than in isolated atomic nuclei. When the density increases to $\sim 4 \times 10^{11}$ g cm^{-3} (note that saturation nuclear density corresponds to $\rho = 2.8 \times 10^{4}$ g cm^{-3}), the ratio n/p reaches a critical level. Any further increase in the density leads to 'neutron drip', that is, a two-phase system in which electrons, nuclei, and free neutrons coexist and together determine the state of lowest energy. Increasing the density above 4×10^{11} g cm^{-3} leads to higher n/p ratios and more and more free neutrons. Finally, when the density exceeds about 4×10^{12} g cm^{-3}, more pressure is provided by neutrons than by electrons (Shapiro and Teukolsky (1983)).

Pulsars are astronomical objects emitting periodic pulses of radio waves. It is thought that the objects are neutron stars. The near simultaneous discoveries of the Crab and Vela pulsars (Hewish *et al.* (1968), Gold (1969)), provided evidence for the formation of neutron stars in supernova explosions. At the relatively low temperatures ($\leq$keV) expected for all but the youngest neutron stars, one expects to find neutron superfluidity in the crust and interior (see Fig. 1.16). One also expects the remaining protons in the interior to be paired and hence

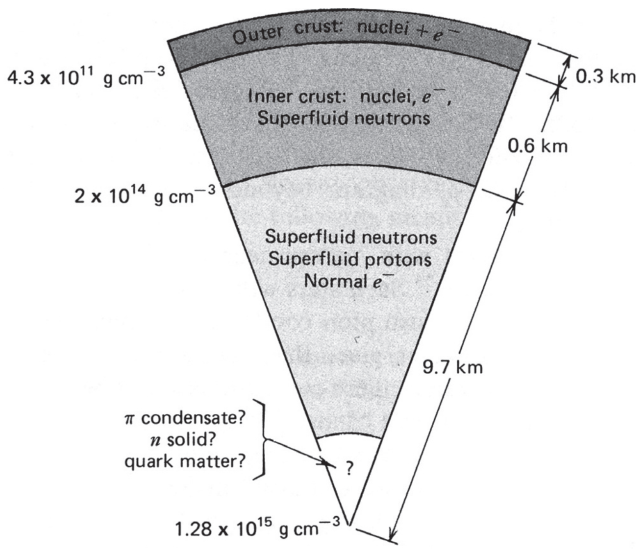

Figure 1.16. Cross-section of neutron stars (after Pines (1980)).

https://doi.org/10.1017/9781009401920.002 Published online by Cambridge University Press

superconducting (Shaham (1980)). It is unlikely, however, that the electrons are superconducting because the electron–phonon coupling is too weak.

Calculations suggest that at least three distinct hadronic superfluids exist inside a neutron star (Pines *et al*. (1980)):

1. In the inner crust ($4.3 \times 10^{11}\,\mathrm{g\,cm^{-3}} < \rho < 2 \times 10^{14}\,\mathrm{g\,cm^{-3}}$, the free neutrons may pair in a ${}^1S_0$ state to form a superfluid amid the neutron-rich nuclei.
2. In the quantum liquid regime ($\rho \geq 2 \times 10^{14}\,\mathrm{g\,cm^{-3}}$), where the nuclei have dissolved into a degenerate fluid of neutrons and protons, the neutron fluid is likely to be paired in a ${}^3P_2$ state.
3. The protons in the quantum liquid are expected to be superconducting in a ${}^1S_0$ state.

There are a number of important consequences of hadron superfluidity and superconductivity, which may lead to observational effects. In particular the cooling time scale of pulsars (Pizzochero *et al*. (2002)), as well as the sudden changes in the pulsar periods known as glitches (Anderson *et al*. (1982), Pines, Tamagaki and Tsuruta (1992)).

https://doi.org/10.1017/9781009401920.002 Published online by Cambridge University Press